Supporting Information

Carbon Nitride Hollow Theranostic Nanoregulators Executing Laser-Activatable Water Splitting for Enhanced Ultrasound/Fluorescence Imaging and Cooperative Phototherapy

Xing Zhang[1,3], Jeremiah Ong'achwa Machuki[1], Wenzhen Pan[1], Weibing Cai[1], Zhongqian Xi[1], Fuzhi Shen[1], Lijie Zhang[4], Yun Yang[4], Fenglei Gao[1,] and Ming Guan[2,*]*

1. Jiangsu Key Laboratory of New Drug Research and Clinical Pharmacy, Xuzhou Medical University, Xuzhou, Jiangsu 221002, People's Republic of China.
2. Department of Laboratory Medicine, Huashan Hospital, Fudan University, Shanghai 200040, People's Republic of China.
3. Department of Trauma and Reconstructive Surgery, RWTH Aachen University Hospital, Aachen 52074, Germany.
4. Nanomaterials and Chemistry Key Laboratory, Wenzhou University, Wenzhou, Zhejiang 325027, People's Republic of China.

*Corresponding author email address: jsxzgfl@sina.com (F. Gao), guanming88@yahoo.com (M. Guan).

Contents

Reagents and Materials

Dimethyl Formamide (DMF), graphene oxide (GO), tetrachloroauric (III) acid ($HAuCl_4 \cdot 3H_2O$), ascorbic acid (AA), Cetyltrimethylammonium bromide (CTAB), and tetraethyl orthosilicate (TEOS) were obtained from Sigma-Aldrich (USA). Cyanamide, absolute ethanol, and methanol were purchased from Aladdin Chemistry, Co., Ltd. (Shanghai, China). Cell counting kit assay kit (CCK-8), Singlet Oxygen Sensor Green reagent (SOSG), 2',7'-Dichlorodihydrofluorescein diacetate (DCFH-DA) and Live-Dead Cell Staining Kit were obtained from Beyotime Institute of Biotechnology (Shanghai, China). DMEM and FBS were obtained from Gibco BRL (Carlsbad, CA, USA).

Nanoparticle Characterization

TEM (FEI Tecnai G2 Spirit Twin, Holland), UV–vis–NIR spectrophotometer (GENESYS 10S, Thermofisher), confocal laser scanning microscope (FV10i, Olympus, Japan), X-ray diffractometer (Bruker D8 Advance), X-ray photoelectron spectrometer (Thermo Scientific Escalab 250Xi), micromeritics instrument (ASAP2020) and Bio-Rad 680 microplate reader were utilized to characterize the synthesized nanoparticles. Besides, the detection of singlet oxygen was based on SOSG and DCFH-DA probe. The photothermal performance of the nanoparticles was evaluated using IR thermal camera (Fotric 225). Moreover, the intracellular O_2 levels were measured using a RDPP probe.

Materials Preparation

N-GQD Preparation

Nitrogen-doped graphene quantum dots (N-GQDs) were synthesized *via* a hydrothermal method, in which nitrogen derived from DMF was tightly bound to GQDs with a strong electron-denoting

effect. The resulting N-GQDs were dialyzed to completely remove impurities of various molecular weights.

N-GQD@HMSN Preparation

Uniform N-GQD@HMSNs were synthesized as previously described with some modifications.[S1,S2] Firstly, StÖber method was utilized to synthesize 100 nm $dSiO_2$. Typically, 17.85 mL of absolute ethanol was mixed with 2.5 mL of N-GQDs suspension, 0.39 mL of aqueous ammonia and 1 mL of TEOS, and reacted at room temperature under magnetic stirring for 1 h. Subsequently, the $dSiO_2$ nanoparticles were centrifuged and rinsed with ethanol, and dispersed in 10 mL double distilled water. At this time, N-GQD is firmly adsorbed on the surface of $dSiO_2$. Secondly, 2 g of CTAC and 200 μL (0.1 g/mL) of TEA solution were dissolved in 18 g of double distilled water, and stirred at 700 rpm/min for 1.5 h to obtain a white turbid liquid. Next, 10 mL of the solution obtained in the first step was added, and continuously stirred for 1 h. Immediately thereafter, 135 μL of TEOS (30 μL/min) was injected using a microinjection pump, and reacted at 80 °C for 1 h. Thirdly, the temperature of the water bath was lowered to 50 °C, and $dSiO_2$ was etched with 0.63 g of Na_2CO_3 for 45 min to obtain N-GQD@HMSNs. The as-prepared nanoparticles were centrifuged and rinsed with a 1 wt% sodium chloride-methanol solution at least 5 times to remove excess CTAC.

N-GQD@HMSN@C_3N_4 Preparation

To incorporate C_3N_4 shell, N-GQD@HMSN nanospheres were used as a template to synthesize N-GQD@HMSN@C_3N_4. Briefly, 4 g of N-GQD@HMSN nanoparticles were added into 10 mL cyanamide with continuous ultrasonic vibration for 2 h at 50 °C. Afterwards, the mixture was stirred at 500 rpm for 10 h in an oil bath with 60 °C. The resultant N-GQD@HMSN@C_3N_4 nanoparticles were collected through centrifugation, washed thrice with ethanol and dried in a

vacuum.

Preparation of P-PEG-RGD-modified N-GQD@HMSN@C_3N_4

First, the P-PEG-RGD polymer was prepared *via* a solid-phase approach. Subsequently, 0.5 mL of polymer solution (1 mg/mL) was added to 15 mL N-GQD@HMSN@C_3N_4 suspension (0.8 mg/mL), and continute to stir for 30 min. After subjecting to ultrasonic treatment of 1 h, the mixed solution was centrifuged and washed with deionized water several times to obtain precipitate. Finally, the obtained precipitate was further lyophilized to collect the final product (R-NCNP) for further use.

Pharmacokinetic Study

In pharmacokinetic study, 4T1 tumor-bearing nude mice were intravenously administered with 200 μL at the R-NCNP dose of 2 mg/mL. At designated time intervals (*i.e.* 0, 1, 2, 4, 8, 12, and 24 h), 10 μL blood were collected and dispersed into 990 μL physiological saline and then melted by chloroazotic acid. After i.v. injection for 24 h, all mice were sacrificed and the tumors and other major organs were collected. In the end, the Si amount of the collected blood and tissue samples were measured by ICP-OES. Data were presented as % ID g^{-1} (mean ± standard deviation (SD)).

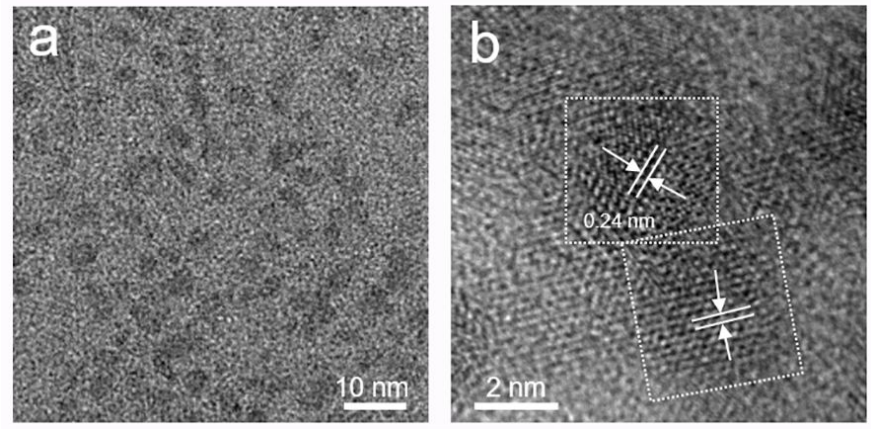

Figure S1. Characterization of as-synthesized N-GQDs. (a) TEM image of monolayer N-GQD; (b) HRTEM image with measured lattice spacing of N-GQD;

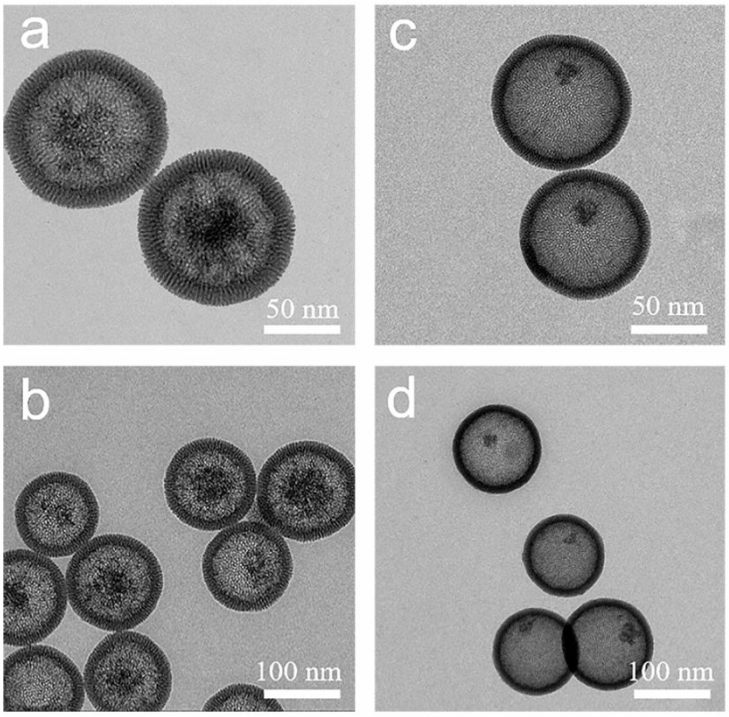

Figure S2. TEM images of fabricated N-GQD@HMSN with high concentration N-GQD (a, b) and low concentration N-GQD (c, d).

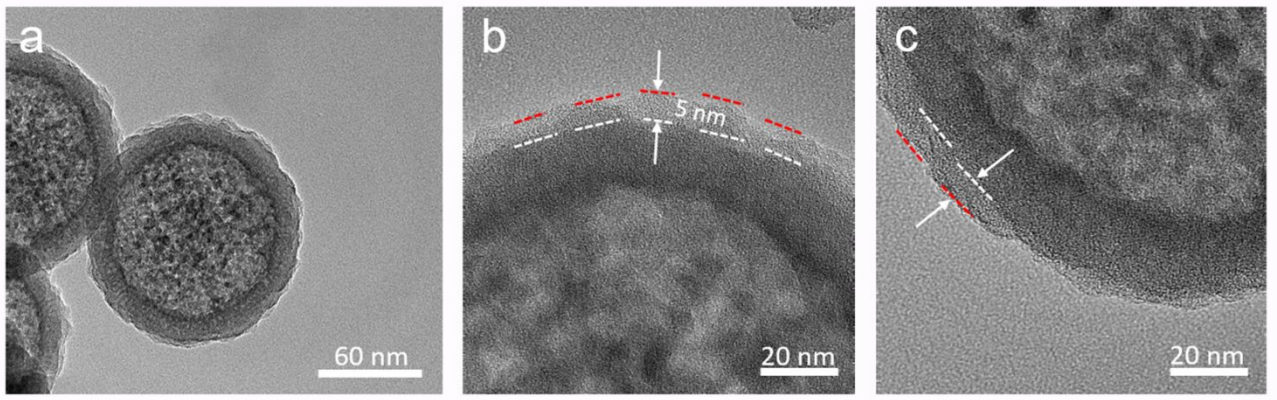

Figure S3. (a) Representative TEM image of as-prepared R-NCNP; (b) and (c) HRTEM images of R-NCNP with C_3N_4 thickness of about 5 nm;

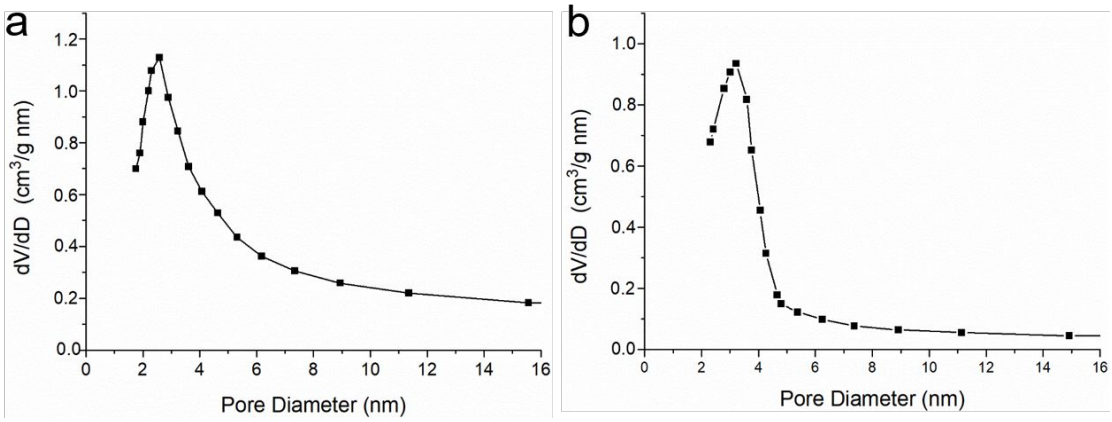

Figure S4. The corresponding pore size distribution of NCN (a) and R-NCNP (b) nanoparticles.

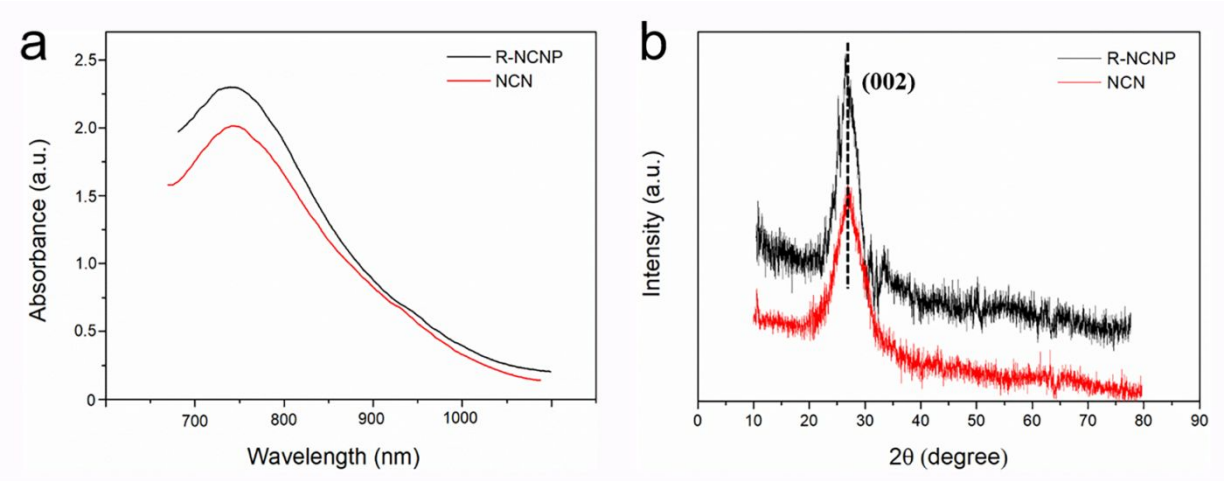

Figure S5. (a) UV−Vis−NIR absorption spectra of the the R-NCNP and NCN NPs aqueous dispersion with 100 μg/mL. (b) XRD patterns of the R-NCNP and NCN NPs.

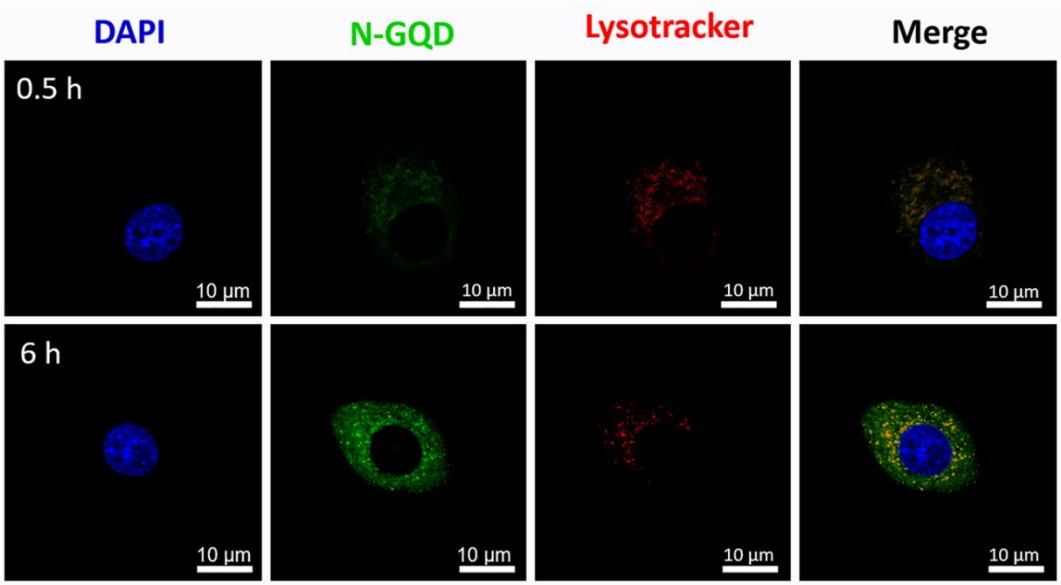

Figure S6. Intracellular localization of R-NCNP NPs incubated with 4T1 cells for 0.5 h and 6 h, respectively. The nuclei were stained with DAPI and the endosomes were marked with LysoTracker Red. Scale bar: 10 μm.

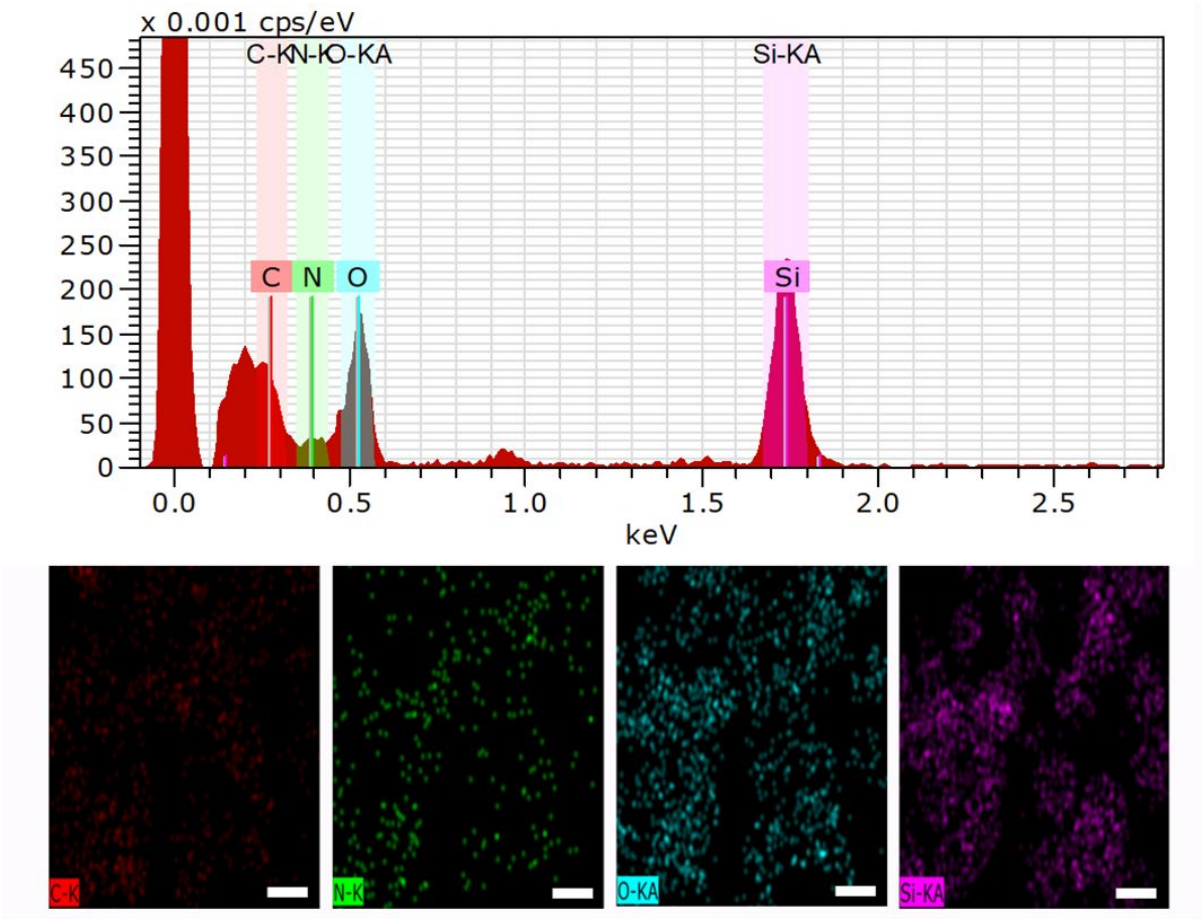

Figure S7. ESD element analysis and EDS elemental mapping of R-NCNP NPs in cells.

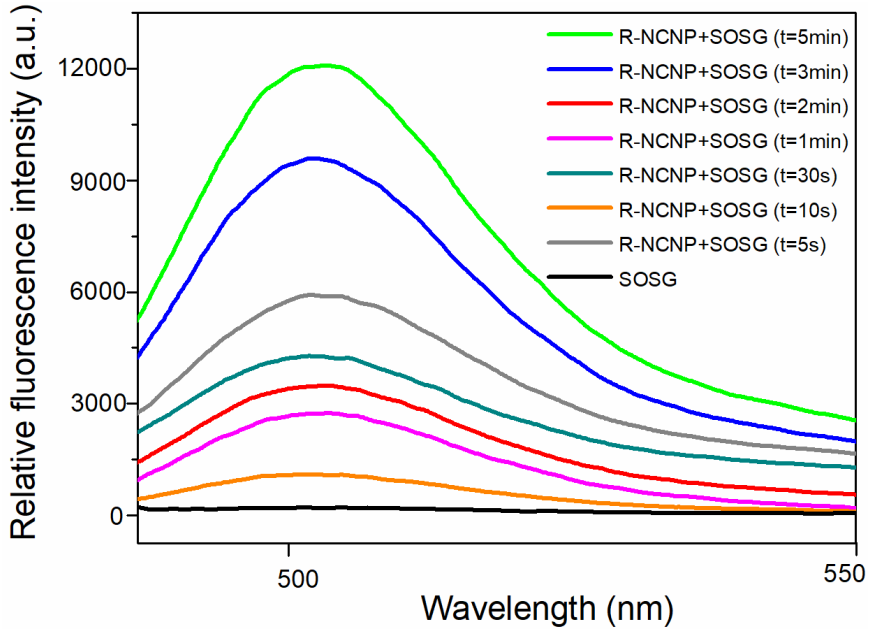

Figure S8. Absorption spectra of SOSG solution containing R-NCNP NPs under various irradiation time with a 635 nm laser, SOSG alone was used as the control.

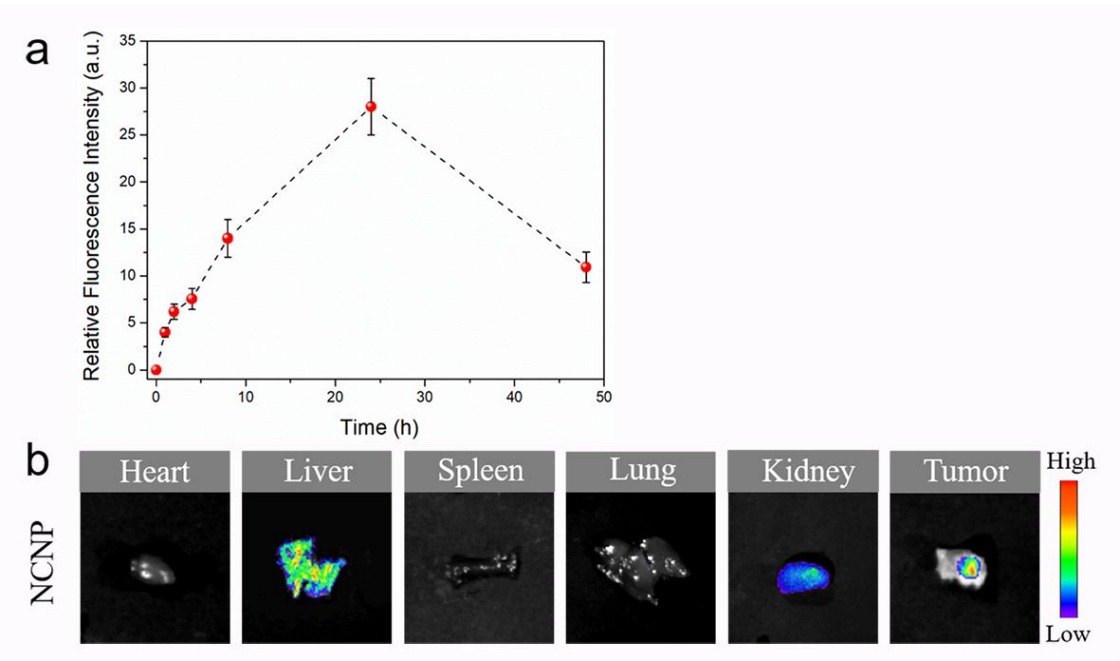

Figure S9. (a) Relative fluorescence intensity of 4T1 tumor tissues obtained at pre-determined time points (0, 1, 2, 8, 24, and 48 hours) after intravenous injection of R-NCNP nanoparticles. (b) The *ex vivo* fluorescence imaging performed for major organs and tumors after 24 h injection of nanosystems devoid of the RGD peptide (NCNP).

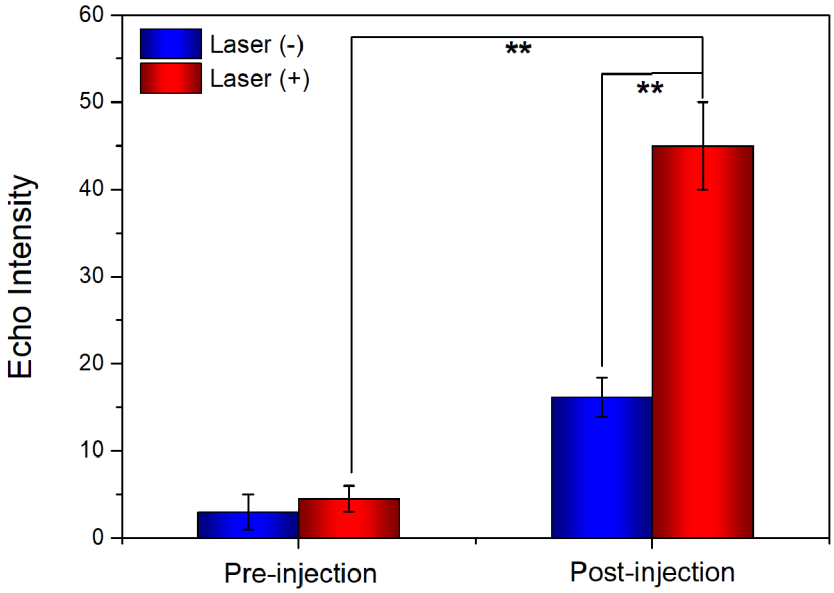

Figure S10. Relative echo intensity of tumor tissue before and after laser irradiation in the B-mode . The difference is statistically significant (**$p < 0.01$).

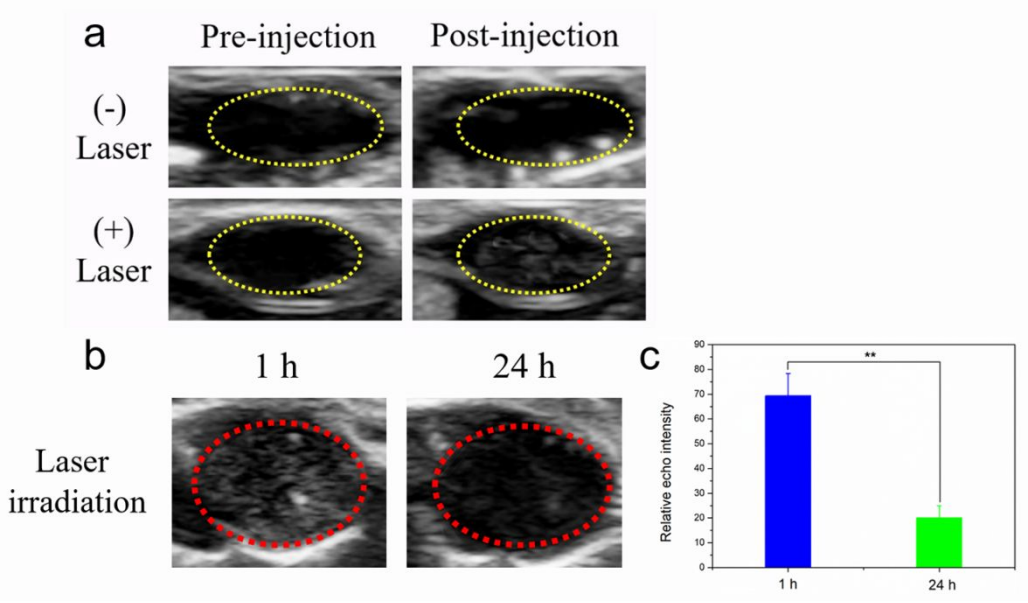

Figure S11. (a) *In vivo* ultrasound images of tumor areas before and after Nm NPs injection without or with laser irradiation. (b) *In vivo* US images of tumors areas after R-NCNP NPs injection at 1 h and 24 h. (c) the corresponding relative echo intensity of (b).

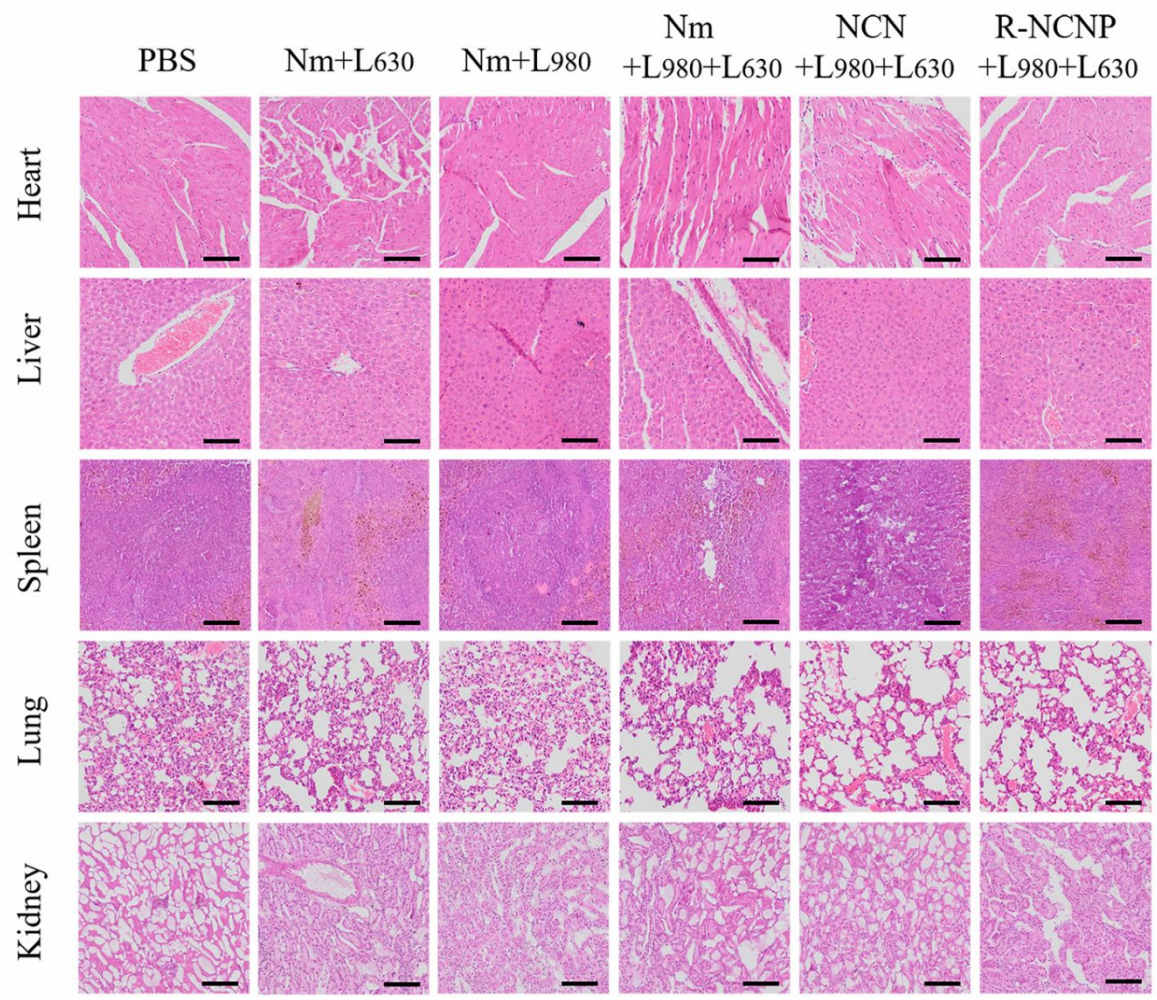

Figure S12. H&E staining of major organs resected from sacrificed mice in various groups after various treatments for 30 days. Scale bars: 50 μm.

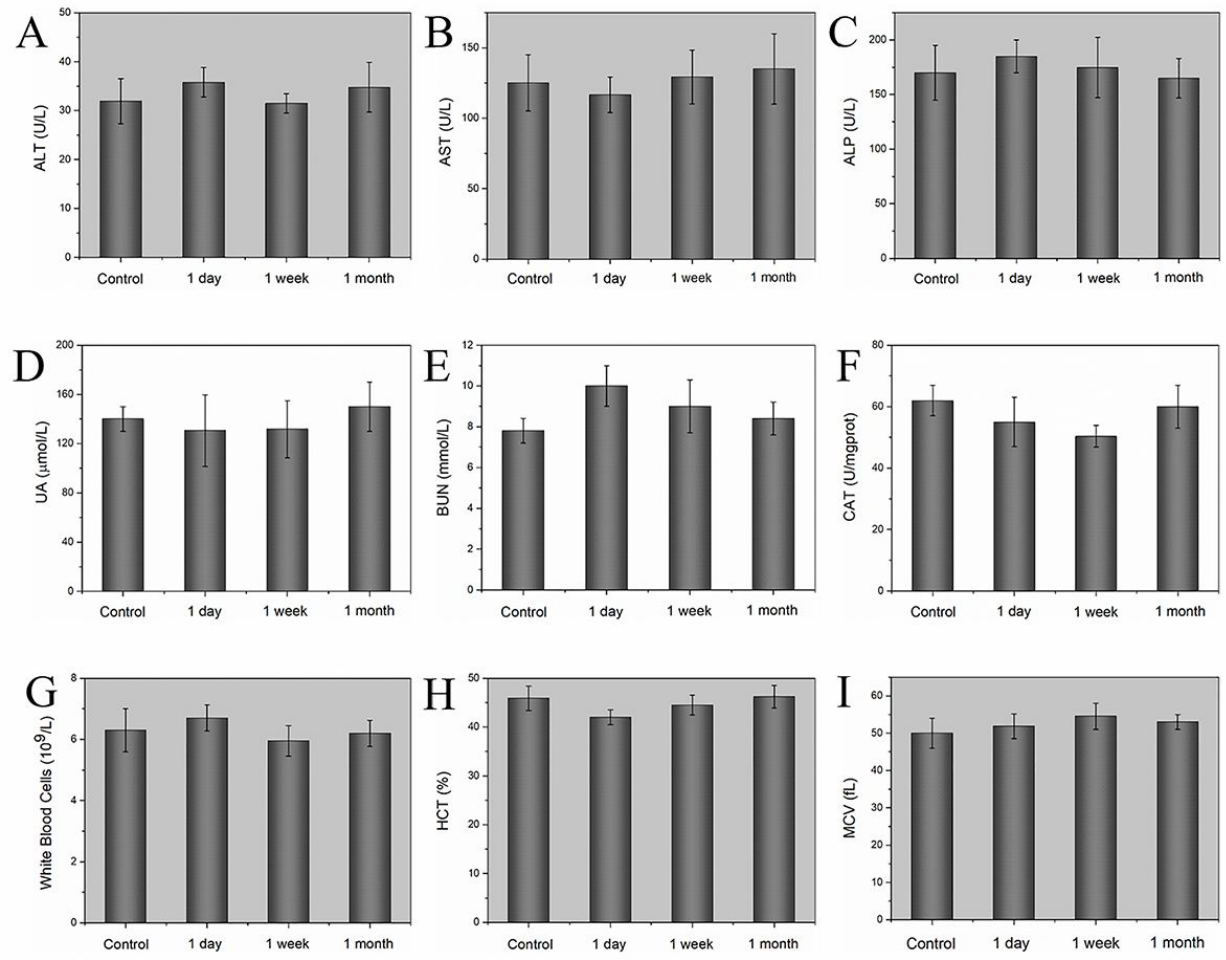

Figure S13. *In vivo* long-term toxicity of R-NCNP NPs after intravenously injection. The hepatic and renal function markers including (A) ALT, (B) AST, (C) ALP, (D) UA, (E) BUN, (F) CAT. And the routine blood examination involving blood levels of (G) WBC, (H) HCT, and (I) MCV for mice treated with R-NCNP at a dose of 30 mg kg^{-1} at indicated time points. Untreated healthy mice served as the control.

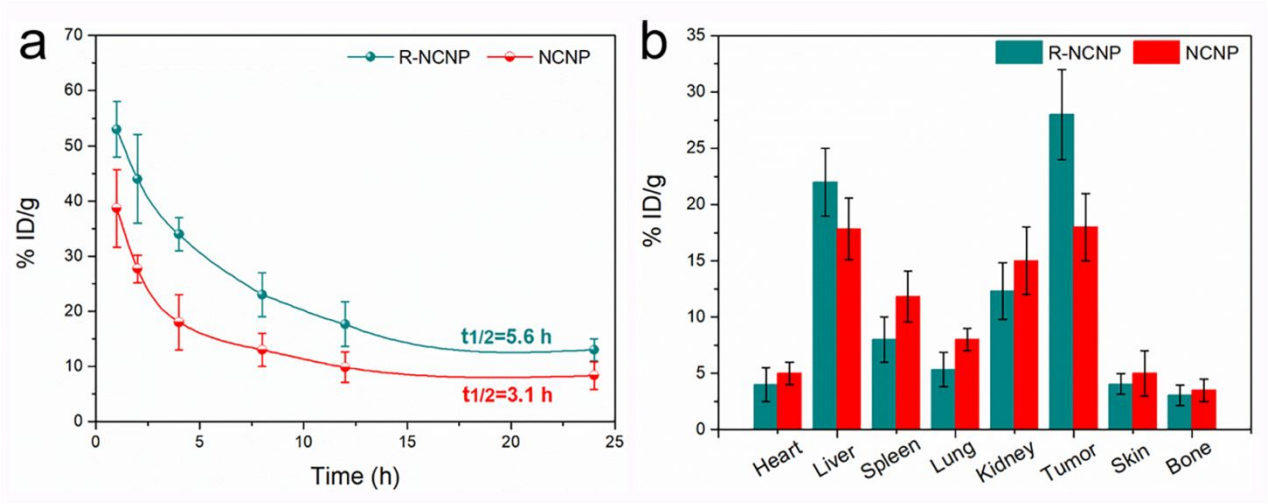

Figure S14. (a) Blood pharmacokinetics of R-NCNPs and NCNPs within 4T1 tumor-bearing mice after i.v. injection. (b) The biodistribution of Si amounts in different organs and tumors of mice collected at 24 h after injection of R-NCNPs and NCNPs through ICP-OES analysis..

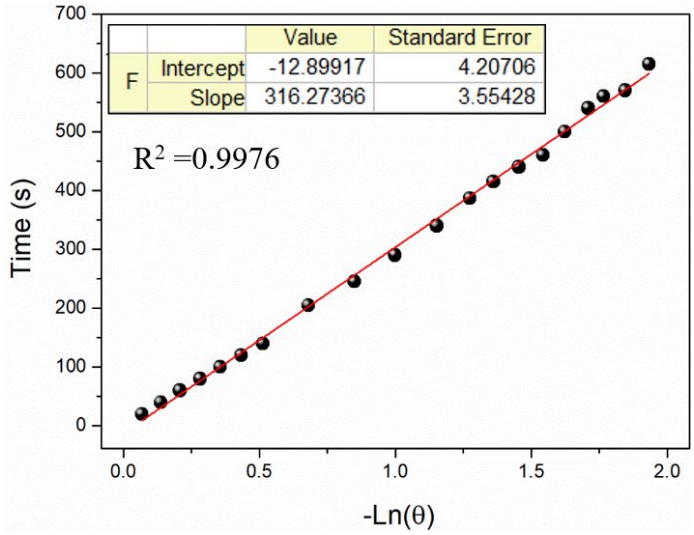

Figure S15. Plot of cooling time as a function of the negative natural logarithm of the temperature driving force obtained from a cooling stage. The time constant, τs, is determined to be 316 s.

The photothermal conversion efficiency (η) of N-GQDS was calculated with the following **EQ 1**.

$$\eta = \frac{hS\,(T_{max} - T_{surr}) - Q_{dis}}{I\,(1 - 10^{-A_{980}})}$$

EQ1

In the equation 1, h is the heat transfer coefficient of the nanocomposites, S is the area cross section

of irradiation, T_{max} and T_{Surr} are the equilibrium temperature and ambient temperature of the surroundings, respectively. Q_{dis} is heat dissipated from light absorbed by the quartz sample cell itself, I is the incident laser power (1.0 W cm^{-2}) and A_{980} is the optical absorbance of the N-GQDs at wavelength of 980 nm. Because the value of hS remains unknown, a dimensionless driving force temperature (θ) is introduced to calculate the value of hS using the following equations:

$$\theta = \frac{T - T_{surr}}{T_{max} - T_{surr}} \qquad \textbf{EQ 2}$$

At the cooling stage of the aqueous dispersion, the cooling time t and abide by the following equation, time constant (τs) for heat transfer from the system could be determined τs =316 s by applying the linear time data from the cooling period *versus* negative natural logarithm of driving force temperature (**Figure S15**).

$$t = -\tau s \ln\theta \qquad \textbf{EQ 3}$$

$$\tau s = \frac{\sum m_i C_{p,i}}{hS} \qquad \textbf{EQ 4}$$

Where m_i and $C_{p,i}$ are the mass (0.45 g) and heat capacity (4.2 J g^{-1}) of deionized water, respectively. In addition, Q_{dis} was measured independently to be 8.4 mW, the (T_{max}-T_{Surr}) was 27.8 °C according to **Figure 2D**, I was 1.0 W cm^{-2}, A_{980} was the absorbance (0.352) of R-NCNP NPs at 980 nm (**Figure S5(A)**).On the basis of the **EQ2**, **EQ3** and **EQ4**, the value of hS is deduced to be 5.98 mW/°C. Substituting 5.98 mW/°C of the hS into **EQ1**, the 980 nm laser heat conversion efficiency (η) of R-NCNP NP can be calculated to be 28.6%.

Reference

[S1] Chen, F.; Hong, H.; Shi, S.; Goel, S.; Valdovinos, H. F.; Hernandez, R.; Theuer, C. P.;

Barnhart, T. E.; Cai, W. Engineering of Hollow Mesoporous Silica Nanoparticles for Remarkably Enhanced Tumor Active Targeting Efficacy. *Sci. Rep.* **2014**, *4*, 5080.

[S2] Goel, S.; Ferreira, C. A.; Chen, F.; Ellison, P. A.; Siamof, C. M.; Barnhart, T. E.; Cai, W. Activatable Hybrid Nanotheranostics for Tetramodal Imaging and Synergistic Photothermal/Photodynamic Therapy. *Adv. Mater.* **2017**, *30*, 1704367.